Spark Ignition Engine Idle Speed Control: An Adaptive Control Approach

Yildiray Yildiz, *Member, IEEE,* Anuradha M. Annaswamy, *Fellow, IEEE,* Diana Yanakiev, *Member, IEEE,* Ilya Kolmanovsky, *Fellow, IEEE*

Abstract

The paper presents an application of a recently developed Adaptive Posicast Controller (APC) for time-delay systems to the Idle Speed Control (ISC) problem in Spark Ignition (SI) Internal Combustion (IC) engines. The objective is to regulate the engine speed to a prescribed set-point in the presence of accessory load torque disturbances such as due to air conditioning and power steering. The adaptive controller, integrated with the existing proportional spark controller, is used to drive the electronic throttle actuator. We present both simulation and experimental results demonstrating the performance improvement by employing the adaptive controller. We also present the modifications and improvements to the controller structure which were developed during the course of experimentation to solve specific problems. In addition, the potential for the reduction in calibration time and effort which can be achieved with our approach is discussed.

Index Terms

Road vehicles, internal combustion engines, adaptive control, delay effects

I. Introduction

The basic problem of Idle Speed Control (ISC) is to maintain the engine speed at a prescribed set-point in the presence of various disturbances such as due to air conditioning, transmission engagement or power steering accessory load torques [1]. There are several well-known challenges

Yildiray Yildiz and A. M. Annaswamy are with the Department of Mechanical Engineering, Massachusetts Institute of Technology, Cambridge, MA, 02139 USA (e-mail: yildiray.yildiz@nasa.gov, aanna@mit.edu).

Diana Yanakiev and Ilya Kolmanovsky are with the Research and Innovation Center, Ford Motor Company, Dearborn, MI, 48121 USA (email: dyanakie@ford.com, ikolmano@ford.com).

in this control problem, one of the most important of which is the time-delay between the intake event and combustion event of the engine. This time delay limits the achievable performance in the electronic throttle control loop. The second challenge is that the controller performance must be robust to changes in the idle speed set-point, to changes in operating conditions (varying altitude, engine temperature and/or ambient temperature, etc.) and to part-to-part and aging-caused variability. Finally, obtaining an accurate and simple model which is appropriate for control design can be both difficult and time-consuming.

Idle Speed Control has been a classical problem in automotive control, and the celebrated Watt's governor (1796) was, in fact, a speed controller for a steam engine. Even though ISC is implemented in most of the vehicles on the road today, increasingly stringent regulatory and customer requirements necessitate its continuing improvement. For instance, a better performing ISC can improve fuel economy by reducing spark reserve and lowering idle speed set-point, and it can also accommodate changes in sensors and actuators (e.g., a replacement of an air-bypass-valve by the electronic throttle or reduction in sensor or actuator cost). Finally, ISC designs that can lower calibration time and effort can help reduce time-to-market, which is a key priority for automotive manufacturers.

The ISC problem is typically addressed by combining some form of a feed-forward control with a closed-loop compensation based on the engine speed error. The feed-forward controller may consist of multiple look-up tables which may, for instance, predict the loads due to accessories for different operating conditions. A closed-loop controller determines the compensation with electronic throttle and spark timing actuators for the engine speed tracking error and is typically gain-scheduled on operating conditions where nonlinear maps are used to determine the gains. The major effort in the calibration, which is the process of determining the appropriate entries in the look-up tables, is spent in determining the gains of the feed-forward controller. One of the main reasons for this may be due to the inadequacy of the closed loop controller, which in turn shifts the burden of compensation to the feed-forward controller.

Many different closed loop designs have been proposed in the literature including $\mathcal{H}_\infty$ control [2], $\mathcal{H}_2$ control [3], sliding mode control [4], [5], ℓ_1 optimization [6], feedback linearization [7], proportional-integral (PI) and proportional-integral-derivative (PID) control [8], [9], [10], [11], [12], linear quadratic control (LQ) [13], [11], [14], model predictive control (MPC) [15], adaptive control [16], [17], [18] and estimation based control [19], [20], [21], to name a few.

A comparison between different control algorithms for the idle speed control problem can be found in [22]. A comprehensive survey of engine models and control strategies developed for ISC can be found in [1].

Literature, given above, about classical and advanced control applications to the ISC problem proves the success of an automatic, model based control approach, and our work built upon these results by eliminating the need of a precise engine model for classical or optimization based algorithms and by eliminating the conservatism introduced by the robust control approaches. This is achieved by using the Adaptive Posicast Controller (APC) [23], [24], which is an adaptive controller for time delay systems. Successful adaptive control approaches are presented also in references [16], [17], [18], but our approach is different from them: In [16], the adaptation is used to select the idle speed set point and in [17], the torque differences among the cylinders are estimated to reduce the short term fluctuations caused by them. Finally, in [18], simulation results of idle speed control by online estimation of the plant parameters and using these estimates in the control scheme using two actuators, spark and bypass valve, are given. In our approach, we apply APC, a model reference adaptive controller developed for time delay systems, to control the idle speed at a prescribed set-point, in the presence of external disturbances like power steering disturbance, and uncertainties due to modeling inaccuracies and operating point changes. We do not employ an online parameter estimation algorithm which may require additional computation power. In addition, we present experimental results showing the success of the algorithm over the baseline controller existing in the vehicle, as well as the robustness of the algorithm by showing the parameter evolution during the course of the experiment.

The authors have previously published preliminary results of APC application to ISC and fuel-to-air ratio control problems in conference papers [25], [26] and [27]. This paper expands on those results with further theoretical improvements, new experimental results and more detailed explanations of the experimental issues. The APC approach addresses the key challenges due to uncertainties and time delay that are important for ISC application. The underlying control architecture includes several components including the classical Smith Predictor [28], its variant reported in [29] based on finite-spectrum assignment, and adaptation [30], [31]. The controller is modified from its original design to take care of the specific needs of the idle speed control application and additional design methods are developed to facilitate the controller development: Firstly, an adaptive feed-forward term is added which is crucial for disturbance

rejection. Secondly, an algorithm is developed for the adaptation rate selection. Thirdly, a fine-tuning method is introduced to minimize the controller tuning. Finally, a robustifying scheme is used to prevent the drift of the adaptive parameters. Our main contribution is the demonstration of the potential of this adaptive controller to improve the performance and to reduce the time and effort required for the controller calibration. This is achieved by the help of modifications and improvements that are listed above.

The experimental results obtained using Ford F-150 test vehicle are repeated. These results demonstrate the capability of the controller to improve performance and decrease the calibration time and effort.

Adaptive Posicast ISC approach represents a step towards a fully self-calibrating ISC because less reliance on feed-forward characterization of accessory loads is required, and because the controller gains are automatically tuned online.

While our control approach is adaptive, its development both benefits from and depends on the structural properties of the underlying plant model. This plant model for ISC control is briefly discussed next, while the reader is referred to [32] for a more extended treatment of the underling modeling techniques.

II. Plant Model

The plant model for ISC explained in this section is standard [32]. The control input in the model is the throttle position in degrees and the output is the engine speed in revolutions-per-minute (rpm). Below, the modeling aspects are discussed for each subsystem.

A. Throttle Mass Flow

The air mass flow thorough the throttle opening during idling can be modeled using the choked flow equation

$$\varpi_{\rm th} = A_{\rm th}\frac{p_{\rm a}}{\sqrt{2RT_{\rm a}}} \tag{1}$$

where, $\varpi_{\rm th}$ is the air mass flow rate passing thorough the throttle opening, $A_{\rm th}$ is the effective area of the throttle, $p_{\rm a}$ is the ambient pressure, $T_{\rm a}$ is the ambient temperature and R is the gas constant. Note that the throttle area is a nonlinear function of the throttle position, but given that during idling the throttle movement is very small, a linear relationship between throttle position and throttle effective flow area can be assumed.

B. Intake Manifold

Assuming isothermal conditions, the intake manifold pressure dynamics can be modeled as

$$\frac{d}{dt}p_{\mathrm{m}} = \frac{RT_{\mathrm{m}}}{V_{\mathrm{m}}}(\varpi_{\mathrm{th}} - \varpi_{\mathrm{eng}}) \tag{2}$$

where, p_{m}, T_{m}, and V_{m} are the manifold pressure, temperature and volume respectively and ϖ_{eng} is the air mass flow rate exiting the intake manifold and entering the engine.

C. Engine Air Mass Flow

The mean value of the fuel-air mixture flow rate entering the engine cylinders can be approximated using the following equation:

$$\varpi_{\mathrm{mix}} = \eta_{\mathrm{v}}\frac{p_{\mathrm{m}}}{RT_{\mathrm{m}}}\frac{V_{\mathrm{d}}\omega_{\mathrm{e}}}{4\pi} \tag{3}$$

where, η_{v} is the volumetric efficiency, V_{d} is the displacement volume and ω_{e} is the engine speed in radians-per-second. Air mass flow rate entering the cylinders can be found using the formula $\varpi_{\mathrm{eng}} = \varpi_{\mathrm{mix}}/[1 + \Phi(F/A)_{\mathrm{s}}]$, where $(F/A)_{\mathrm{s}}$ and Φ represent the stoichiometric fuel-to-air ratio and fuel-to-air ratio normalized by the stoichiometric fuel-to-air ratio, respectively. Φ is referred to as the equivalence ratio.

D. Torque Generation

In general, generated torque is a nonlinear function of engine speed, mass flow rate into the engine cylinders, equivalence ratio and spark advance:

$$T_{\mathrm{e}} = f(N, \varpi_{\mathrm{mix}}, \Phi, SA) \tag{4}$$

where SA represents the spark advance. This nonlinear relationship can be found with a least squares method using engine data. Also note that the induction to power (IP) delay enters into system dynamics through (4) as the torque depends on the delayed value of the mass flow rate into the engine cylinders.

E. Engine Rotational Dynamics

The equation of engine rotational dynamics is as follows:

$$\frac{d}{dt}\omega_{\mathrm{e}} = \frac{1}{J}(T_{\mathrm{e}} - T_{\mathrm{l}}) \tag{5}$$

where, J is the engine inertia in neutral and T_{l} is the load torque on the engine including the internal engine friction.

F. Final Model for ISC

For ISC design, a nonlinear mean value engine model based on the above subsystem models was linearized around the nominal idle speed value (650 rpm) to obtain a linear plant model. Considering the deviation in the throttle position in degrees as the input and the deviation in engine speed in rpm as the output, the parametric transfer function of this linear model was

$$G(s) = K\frac{s^2 + n_1 s + n_2}{s^3 + d_1 s^2 + d_2 s + d_3}e^{-0.15s} \tag{6}$$

Note that the delay free part of the transfer function in (6) is third-order and relative degree one. The simplicity of (6) will subsequently be useful in determining the structure of the Adaptive Posicast Controller (APC).

The IP delay at the nominal idle speed of 650 rpm is 90 ms assuming that this delay is the result of 360 degrees of crank rotation or one revolution of the crank shaft. However, it is known that one revolution is only an approximation, since, for example, the maximum torque production does not occur exactly at the top dead center. In addition, the actuator delay and computational delays also contribute to the overall delay value. 150 ms time delay seen in (6) is a combined result of all these effects.

The parameter values for this nominal operating point were $K = 29.8$, $n_1 = 50$, $n_2 = 833$, $d_1 = 21.2$, $d_2 = 51.3$ and $d_3 = 189.5$. One should also note that these parameter values are valid only for the nominal operating point and thus are specific to certain values of engine speed, load torque, ambient pressure, ambient temperature and engine temperature. The input delay is used to approximate the effect of state delay in the model (1)-(5). Bode plots of the plant transfer function (6) with and without the delay, $G(s)$ and $G_0(s)$, are presented in Fig. 1, assuming the nominal parameter values. This figure clearly shows the rapid phase decrease with increasing frequency due to the time delay.

III. APC Design

A. Initial Design

APC is a model reference adaptive controller for systems with known input delay. Below, we summarize the main idea behind the APC. The the reader is referred to [24] for additional details. Consider a linearized plant with input-output description given as

$$y(t) = W_{\rm p}(s)u(t-\tau), \qquad W_{\rm p}(s) = \frac{k_{\rm p}Z_{\rm p}(s)}{R_{\rm p}(s)} \tag{7}$$

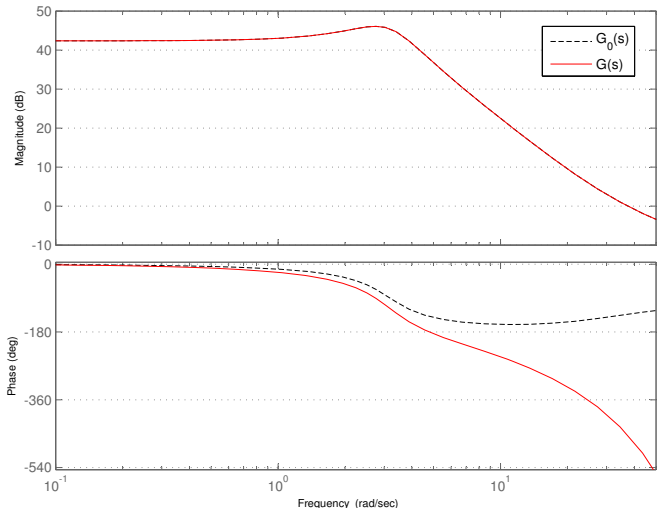

Fig. 1. Bode plots of $G(s)$ and $G_0(s)$

where y is the measured plant output, u is the control input, and $W_{\rm p}(s)$ is the delay-free part of the plant transfer function. $R_{\rm p}(s)$ is the $n^{\rm th}$ order denominator polynomial, not necessarily stable and the numerator polynomial, $Z_{\rm p}(s)$ has only minimum phase zeros. The relative degree, n^*, which is equal to the order of the denominator minus the order of the numerator, is assumed to be smaller or equal to two. It is also assumed that the delay and the sign of the high frequency gain $k_{\rm p}$ are known, but otherwise $W_{\rm p}(s)$ may be unknown. Suppose that the reference model, reflecting desired response characteristics, is given as

$$y_{\rm m}(t) = W_{\rm m}(s)r(t-\tau), \qquad W_{\rm m}(s) = \frac{k_{\rm m}}{R_{\rm m}(s)} \tag{8}$$

where $R_{\rm m}(s)$ is a stable polynomial with degree n^*, $k_{\rm m}$ is the high frequency gain and r is the desired reference input.

Consider the following state space representation of the plant dynamics (7), together with two "signal generators" formed by a controllable pair Λ, l

$$\dot{x}_{\rm p}(t) = A_{\rm p}x_{\rm p}(t) + b_{\rm p}u(t-\tau), \;\; y(t) = h_{\rm p}^T x_{\rm p}(t) \tag{9}$$

$$\dot{\omega}_1(t) = \Lambda\omega_1(t) + lu(t-\tau) \tag{10}$$

$$\dot{\omega}_2(t) = \Lambda\omega_2(t) + ly(t) \tag{11}$$

where, $\Lambda \in \Re^{nxn}$ and $l \in \Re^n$. It follows [33] that there exist $k^* \in \Re$, α_1^{*T}, $\alpha_2^{*T} \in \Re^n$, $\lambda^*(\sigma)$:

$[-\tau, 0] \rightarrow \Re$ such that the control law

$$\begin{aligned} u(t) &= \alpha_1^{*T}\omega_1(t) + \alpha_2^{*T}\omega_2(t) + \int_{-\tau}^{0} \lambda^*(\sigma)u(t+\sigma)\mathrm{d}\sigma \\ &\quad + k^* r(t). \end{aligned} \tag{12}$$

satisfies the exact model matching condition.

$$\frac{y(t)}{r(t)} = \frac{k_{\mathrm{m}}}{R_{\mathrm{m}}(s)} e^{-\tau s}. \tag{13}$$

We now consider the control of the plant (7) when the transfer function $W_{\mathrm{p}}(s)$ has unknown coefficients and the time delay τ is known. Consider the following adaptive controller [24]:

$$\begin{aligned} u(t) &= \alpha_1(t)^T\omega_1(t) + \alpha_2(t)^T\omega_2(t) + \int_{-\tau}^{0} \lambda(t,\sigma)u(t+\sigma)\mathrm{d}\sigma \\ &\quad + k(t)r(t), \\ \dot{\theta}(t) &= -\Gamma e_1(t)\Omega(t-\tau), \\ \frac{\partial\lambda(t,\sigma)}{\partial t} &= -\gamma_\lambda(\sigma)e_1(t)u(t+\sigma-\tau) \end{aligned} \tag{14}$$

where,

$$\theta = \begin{bmatrix} \alpha_1 \\ \alpha_2 \\ k \end{bmatrix}, \qquad \Omega = \begin{bmatrix} \omega_1 \\ \omega_2 \\ r \end{bmatrix}, \qquad e_1 = y - y_{\mathrm{m}}, \tag{15}$$

Γ is a diagonal matrix, the entries of which represent the adaptation rate of the corresponding controller parameter and $\gamma_\lambda(\sigma)$ is the adaptation rate for the controller parameter $\lambda(t,\sigma)$. Defining the parameter errors as $\tilde{\theta}(t) = \theta(t) - \theta^*$, $\tilde{\lambda}(t,\sigma) = \lambda(t,\sigma) - \lambda^*(\sigma)$, the control signal u in (14) can be rewritten as

$$\begin{aligned} u(t) &= \alpha^{*T}\omega(t) + \int_{-\tau}^{0} \lambda^*(\sigma)u(t+\sigma)\mathrm{d}\sigma \\ &\quad + k^* r(t) \\ &\quad + \tilde{\alpha}(t)^T\omega(t) + \int_{-\tau}^{0} \tilde{\lambda}(t,\sigma)u(t+\sigma)\mathrm{d}\sigma \\ &\quad + \tilde{k}(t)r(t) \end{aligned} \tag{16}$$

where $\alpha \triangleq \left[\begin{array}{cc} \alpha_1 & \alpha_2 \end{array}\right]$. It is shown in [24] that the differential equations, (9), (10), (11) together with the control signal (16) describe the closed loop dynamics as

$$\begin{aligned} \dot{X}_{\rm p}(t) &= A_{\rm m}X_{\rm p}(t) + b_{\rm m}\big[\tilde{\alpha}^T(t-\tau)\omega(t-\tau) \\ &+ \int_{-\tau}^{0} \tilde{\lambda}(t-\tau,\sigma)u(t-\tau+\sigma){\rm d}\sigma + \tilde{k}(t-\tau)r(t-\tau) + k^*r(t-\tau)\big], \\ y_{\rm p}(t) &= h_{\rm m}^T X_{\rm p}(t) \end{aligned} \tag{17}$$

where, $X_{\rm p} \triangleq \left[\begin{array}{ccc} x_{\rm p}^T & \omega_1^T & \omega_2^T \end{array}\right]^T$, $h_{\rm m}^T \triangleq \left[\begin{array}{ccc} h_{\rm p}^T & 0 & 0 \end{array}\right]$, $y_{\rm p} = y$ and $A_{\rm m}$ is a constant Hurwitz matrix. From the model matching condition, we know that when the parameter errors are equal to zero, the closed loop transfer function is identical to that of the reference model. Therefore, the reference model can be described by the $(3n)^{\rm th}$ order differential equation

$$\dot{X}_{\rm m}(t) = A_{\rm m}X_{\rm m}(t) + b_{\rm m}k^*r(t-\tau),\ y_{\rm m}(t) = h_{\rm m}^T X_{\rm m}(t) \tag{18}$$

where,

$$\begin{aligned} X_{\rm m}(t) &\triangleq \left[x_{\rm p}^{*T}\ \ \omega_1^{*T}\ \ \omega_2^{*T}\right]^T, \\ h_{\rm m}^T\left(sI - A_{\rm m}\right)^{-1} b_{\rm m}k^* &= \frac{k_{\rm m}}{R_{\rm m}(s)}. \end{aligned} \tag{19}$$

Note that $x_{\rm p}^*(t), \omega_1^*(t)$ and $\omega_2^*(t)$ can be considered as the signals in the reference model corresponding to $x_{\rm p}(t), \omega_1(t)$ and $\omega_2(t)$ in the closed loop system. Therefore, subtracting (18) from (17), we get an error equation for the overall system as

$$\begin{aligned} \dot{e}(t) &= A_{\rm m}e(t) + b_{\rm m}\big[\tilde{\alpha}^T(t-\tau)\omega(t-\tau) \\ &\quad + \int_{-\tau}^{0} \tilde{\lambda}(t-\tau,\sigma)u(t-\tau+\sigma){\rm d}\sigma \\ &\quad + \tilde{k}(t-\tau)r(t-\tau)\big], \\ e_1(t) &= h_{\rm m}^T e(t). \end{aligned} \tag{20}$$

where $e(t) = X_{\rm p} - X_{\rm m}$ and $e_1(t) = y_{\rm p}(t) - y_{\rm m}(t)$. Equation (20) can be written in a more compact form as

$$\begin{aligned} \dot{e}(t) &= A_{\rm m}e(t) + b_{\rm m}\big[\tilde{\theta}^T(t-\tau)\Omega(t-\tau) \\ &\quad + \int_{-\tau}^{0} \tilde{\lambda}(t-\tau,\sigma)u(t-\tau+\sigma){\rm d}\sigma\big] \\ e_1(t) &= h_{\rm m}^T e(t). \end{aligned} \tag{21}$$

Using the error model (21) and defining an appropriate Lyapunov Krasovskii functional, it can be shown [24] that the plant (7), adaptive controller and the adaptive laws given in (14) have bounded solutions for all $t \geqslant t_0$ and $\lim_{t\to\infty} e_1(t) \to 0$.

B. Implementation Enhancements

In order to apply the Adaptive Posicast Controller specified by (10), (11) and (14), one has to address several issues which were not taken into account during the initial design but arise in the implementation. Below, we explain these issues and how we address them.

1) Disturbance rejection: Controller (14) is a model reference adaptive controller where the goal is to force the plant output follow the reference model output. In the design stage, the input disturbances are not explicitly taken into account. However, in the idle speed application, it can be shown that the controller is rejecting constant input disturbances. Indeed, the reference, idle speed set-point, is constant, which turns the feed-forward term $k(t)r(t)$ into a pure integrator. Please see Appendix A for the proof of the disturbance rejection.

2) Approximation of the finite integral term: The finite integral term in the control signal u given in (14) is implemented by using a set of point-wise delays [29] as in the following:

$$\int_{-\tau}^{0} \lambda(\sigma,t)u(t+\sigma)\mathrm{d}\sigma = \lambda_1(t)u(t-dt) + .. + \lambda_m(t)u(t-mdt) \tag{22}$$

where dt is the sampling interval and $mdt = \tau$. In the experiments $dt = 30$ ms, so $m = 0.15/0.03 = 5$. With this approximation, the adaptive laws given in (14) can be represented as

$$\dot{\bar{\theta}}(t) = -\bar{\Gamma}e_1(t)\bar{\Omega}(t-\tau) \tag{23}$$

where,

$$\bar{\theta} = \begin{bmatrix} \alpha_1 \\ \alpha_2 \\ \lambda_1 \\ \vdots \\ \lambda_m \\ k \end{bmatrix}, \qquad \bar{\Omega} = \begin{bmatrix} \omega_1 \\ \omega_2 \\ u(t-dt) \\ \vdots \\ u(t-mdt) \\ r \end{bmatrix}, \tag{24}$$

and $\bar{\Gamma} > 0$ is a diagonal adaptation rate matrix.

In [34], the limitations of this approximation have been pointed out together with an example of unstable behavior arising due to numerical integration. In the powertrain control problem

considered here, both in the experiments and in the simulations, the values of coefficients λ_{i} are in the order of 10^{-4}, and for these values we have been able to confirm that the danger of the instabilities due to numerical approximation does not arise. In addition, the stability margin for different values of λ_i's is quite large. Please see Appendix C for details.

3) Robustness: The adaptive controller design presented in Section III-A portrayed an idealized situation. The delay free part of the plant dynamics, $W_{\mathrm{p}}(s)$, is assumed to be finite dimensional, linear and time invariant with unknown parameters. It is also assumed that the inputs and outputs to the plant can be measured exactly. However, in the real implementation, no plant is truly linear or finite dimensional. Plant parameters may vary with time and operating conditions, and measurements may be contaminated by noise. The plant model is almost always approximate. It is precisely in these cases that adaptive control is most needed [33].

Due to the above possible violations of the assumptions, the controller parameters may drift without converging to a bounded region. One of the remedies to this problem is using a σ-modification robustness scheme [33], which mainly adds a damping term to adaptation laws. With the σ-modification, the adaptive law given in (23) is modified as

$$\dot{\bar{\theta}}_{\mathrm{i}}(t) = -\bar{\Gamma}_{\mathrm{ii}} e_1(t) \bar{\Omega}_{\mathrm{i}}(t-\tau) - \sigma \bar{\theta}_{\mathrm{i}}(t) \tag{25}$$

where σ is a constant. The drawback of this adaptive law is that the origin is no longer an equilibrium point of (34) and (25). This implies that even when all the assumptions are perfectly satisfied, the errors do not converge to zero. One way to remedy this drawback is to use a conditional σ-modification scheme:

$$\dot{\bar{\theta}}_{\mathrm{i}}(t) = \begin{cases} -\bar{\Gamma}_{\mathrm{ii}} e_1(t) \bar{\Omega}_{\mathrm{i}}(t-\tau) - \sigma \bar{\theta}_{\mathrm{i}}(t) & \text{if} \quad \left|\bar{\theta}_{\mathrm{i}}\right| \geqslant \breve{\bar{\theta}}_i \\ -\bar{\Gamma}_{\mathrm{ii}} e_1(t) \bar{\Omega}_{\mathrm{i}}(t-\tau) & \text{otherwise} \end{cases} \tag{26}$$

where, $\breve{\bar{\theta}}_i$ is a predetermined constant. Although we observed in our vehicle experiments that this method is working well for the idle speed control application, one limitation of this method is a lack of automatic procedure to predetermine the value of $\breve{\bar{\theta}}_i$. Several approaches to selecting $\breve{\bar{\theta}}_i$ have been proposed. Firstly, one may fix the value of $\breve{\bar{\theta}}_i$ as the corresponding controller parameter vector which will satisfy the model matching condition for the worst case uncertainty in the plant parameters. Alternatively, some experiments can be conducted without using σ-modification and the controller parameters can be observed after which a reasonable value for the $\breve{\bar{\theta}}_i$ can be selected depending on these observations. For example, one can observe the values

of $\bar{\theta}_i$ at different operating points and then select a $\breve{\bar{\theta}}_i$ that prevents the $\bar{\theta}_i$ drifting away a certain range of these observed values. Finally, another method might be first setting the initial values of the controller parameters in such a way that model matching is satisfied for nominal plant parameters and then $\breve{\bar{\theta}}_i$ can be set as a certain percentage higher than the absolute value of these initial conditions. In our experiments, we used the second proposed method.

4) Adaptation rate selection: We choose the adaptation gain $\bar{\Gamma}_{\mathrm{ii}}$ for a particular controller parameter $\bar{\theta}_{\mathrm{i}}$ using the following empirical rule

$$\bar{\Gamma}_{\mathrm{ii}} = \frac{\left|(\bar{\theta}_{\mathrm{i}})^*_{\mathrm{e}}\right|}{3\tau_{\mathrm{m}}\left|e_1(t)\bar{\Omega}_{\mathrm{i}}(t-\tau)\right|} \approx \frac{\left|(\bar{\theta}_{\mathrm{i}})^*_{\mathrm{e}}\right|}{3\tau_{\mathrm{m}}(r^*)^2} \tag{27}$$

where $(\bar{\theta}_{\mathrm{i}})^*_{\mathrm{e}}$ is an estimate of the desired control parameter, τ_{m} is the time constant of the reference model and r^* is a characteristic value of the reference signal. The rationale for the above is that the desired speed of adaptation is determined by the value that the parameter $\bar{\theta}_{\mathrm{i}}$ must reach in a time $3\tau_{\mathrm{m}}$, which corresponds to the settling time. Since the assumption is that the plant parameters are unknown, the actual desired control parameter vector, $\bar{\theta}^*_{\mathrm{i}}$, is unknown. $(\bar{\theta}_{\mathrm{i}})^*_{\mathrm{e}}$ used in (27) should therefore be viewed as an estimate of $\bar{\theta}^*_{\mathrm{i}}$ derived from the matching condition using a nominal plant model. It is assumed that the control parameters start from zero, and also that the orders of magnitude of $e_1(t)$ and $\bar{\Omega}_{\mathrm{i}}(t)$ are close to that of the reference signal. This last assumption can be verified at the first few instants of the operation where the error is approximately equal to the reference signal. So, in a sense, the $\bar{\Gamma}_{\mathrm{ii}}$ selection is based on worst condition where adaptation has just begun.

5) Fine-tuning: Equations (22) and (27) imply that $(\bar{\theta}_{\mathrm{i}})^*_{\mathrm{e}}$ and therefore λ^*_{i}, i = 1, 2, .., 15, need to be estimated to determine $\bar{\Gamma}$. Since λ_{i}'s were observed to be small in the simulations, we determined the ideal values of the controller parameters neglecting the delay in the plant and using a pole placement procedure [33]. Also, λ_{i}'s were observed to have the same order of magnitude for all i, which suggests that the same adaptation gain, $\bar{\Gamma}_\lambda$ for λ_{i}, $i = 1, .., 5$ can be used in (23). The value of $\bar{\Gamma}_\lambda$ was determined using simulation studies of the linearized model.

Due to the approximations discussed above, the resulting $\bar{\Gamma}$ may be non-ideal. Therefore, a

weighting matrix M was included as $\bar{\Gamma}_{\mathrm{w}} = \bar{\Gamma} M$ with

$$M = \begin{bmatrix} z_{\mathrm{u}} I_{\mathrm{n}\times\mathrm{n}} & 0 & 0 & 0 \\ 0 & z_{\mathrm{y}} I_{\mathrm{n}\times\mathrm{n}} & 0 & 0 \\ 0 & 0 & I_{\mathrm{m}\times\mathrm{m}} & 0 \\ 0 & 0 & 0 & z_{\mathrm{r}} \end{bmatrix} \tag{28}$$

where, z_{u}, z_{y} and z_{r} are constants that are used to fine-tune the adaptation gains. Extensive simulations and experiments on the F-150 test vehicle revealed that setting $z_{\mathrm{u}} = z_{\mathrm{r}} = 1$ and increasing z_{y} made the system response faster and improved the disturbance rejection performance by decreasing the overshoots and undershoots after introducing/removing the disturbances.

The above discussion implies that the selection of $\bar{\Gamma}$ requires only two free parameters, $\bar{\Gamma}_{\lambda}$ and z_{y} that are to be empirically determined.

6) Anti-windup logic: The actuator, electronic throttle, has its hard limits and the calculated control signal may sometimes exceed these limits, either from below or from above. In the case of idle speed control application, the desired throttle angle is small and thus the saturation may occur due to the control signal hitting the lower limit of the saturation. Consequently, an add-on algorithm needs to be integrated with the controller that prevents the winding up of the integrators resulting from the adaptation laws in (14).

We use anti-windup logic where the main goal is to stop the adaptation if the control signal saturates and if the tracking error, $e_1 = y_{\mathrm{m}} - y_{\mathrm{p}}$, is not favorable. Calling the control signal before the saturation block as u and after the saturation as u_{sat}, the anti-windup algorithm can be expressed as in the following.

$$\dot{\bar{\theta}}_{\mathrm{i}}(t) = \begin{cases} 0 & \text{if} \quad u > u_{\mathrm{sat}} \quad \text{and} \quad e_1 < 0 \\ & \quad \text{or} \\ & u < u_{\mathrm{sat}} \quad \text{and} \quad e_1 > 0 \\ -\bar{\Gamma}_{\mathrm{ii}} e_1(t) \bar{\Omega}_{\mathrm{i}}(t-\tau) & \text{otherwise} \end{cases} \tag{29}$$

The additional tracking error based condition for not suspending the adaptation during saturation improved the speed of the transient response as has been demonstrated in our vehicle experiments.

There are more rigorous anti-windup methods that are specifically developed for adaptive controllers [35]. We plan to apply these methods in our future research.

C. Final Design and Calibration

A control design that is meant to be used in a mass-production application must be accessible and easy to use by the engineers who actually implement and support the control strategy in production. This is important given that these engineers may not be highly skilled and experienced in advanced control methods. Motivated by these considerations, below we give a step by step design procedure to obtain a transparent and streamlined design process. We assume that a linear plant model with uncertain parameters and a known time delay is available.

Step 1. Select Λ and l of the signal generators defined in (10) and (11). These signal generators act like state observers and it is suggested that their eigenvalues are selected much faster than the reference model pole. Note that the Λ-l pair must be controllable.

Step 2. Set the initial value of the controller parameters to zero except for the feed-forward term $k(t)$. It is suggested that this parameter is initialized such that $k(0) \in (0, 1)$

Step 3. Set the time constant of the reference model at least two times faster than that of the nominal plant time constant.

Step 4. Set the adaptation rate matrix Γ according to the algorithm given in (27).

Step 5. Tune the parameter z_{y} until the highest unmeasured load is rejected according to the requirements. Note that increasing z_{y} decreases transient excursions, however higher gains might cause undesired oscillations.

Apart from these five easy steps, the design must be integrated with the robustness scheme presented in (26).

Note that the controller needs only about 0.35KB of memory for the data storage and requires less than 83 number of operations per computation cycle. This corresponds to less than $2.8 \cdot 10^3$ floating point operations per second (flops). For conventional ECU's the APC controller use around 0.028 percent of the total computational power and that is negligible. Please see Appendix B for the calculation of the memory requirements and computational complexity.

IV. Simulations

This section presents the simulation results using the nonlinear engine model. We note that the simulation model was available for a similar but not exactly the same engine as used in the experimental vehicle.

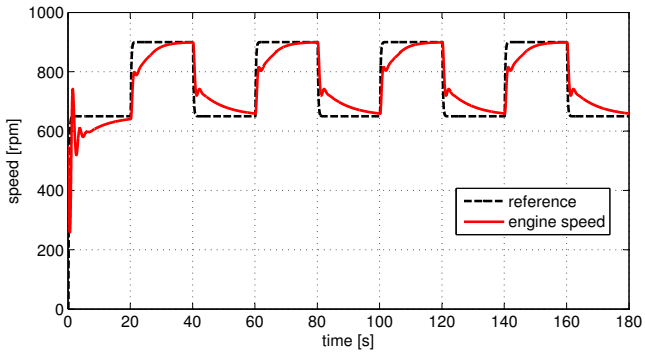

Fig. 2. Nonlinear model set-point tracking. Adaptation rates are calculated using (27) with no further tuning.

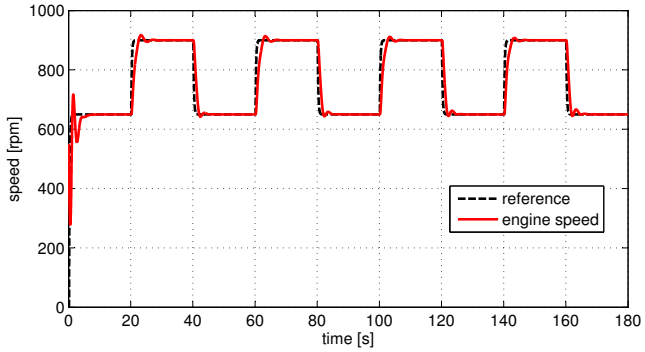

Fig. 3. Nonlinear model set-point tracking. $z_{\mathrm{u}} = z_{\mathrm{r}} = 1$, $z_{\mathrm{y}} = 220$.

Figure 2 shows the response of the nonlinear engine model to step changes in the idle speed set-point. The adaptation rates were calculated setting M = I. Although the response is sluggish, this figure demonstrates that the rule (27) produces reasonable initial estimates for the adaptation rates.

Figure 3 shows the response of the nonlinear model to step changes in the idle speed set-point by changing z_{y} to 220. By changing just this single parameter, the increase in the adaptation gain is attained which provides a much faster yet still well damped response.

All initial conditions for the controller parameters were set to zero except for the feed-forward term $k(t)$. It was found that any value of $k(0)$ chosen from the interval $(0, 1)$ gave a reasonable performance. Results given in the simulations correspond to the case when $k(0) = 0.3$.

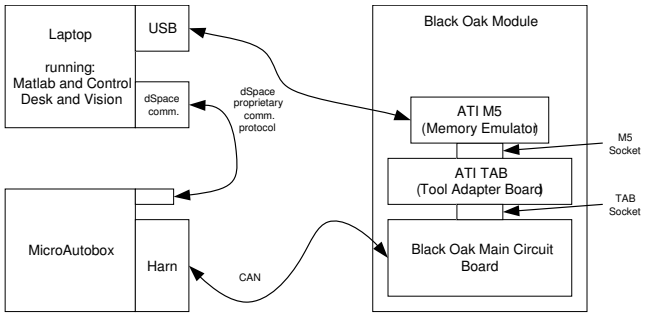

Fig. 4. Rapid prototyping with MicroAutoBox using CAN.

V. EXPERIMENTS

The experimental results given in this section were obtained using an F-150 test vehicle provided by Ford Motor Company. The vehicle has a 4.6 liter V-8 front engine with a multi-port fuel injection system. The engine has two valves per cylinder and can achieve 231 Hp at 4750 rpm and 397 Nm at 3500 rpm. The air intake is controlled with an electronic throttle.

A dSPACE MicroAutoBox, communicating with the engine control unit (ECU) via CAN bus was used for real-time controller rapid prototyping. This system is used to implement the controller and monitor the performance. Figure 4 shows the hardware wiring. In the production environment, the engine is controlled by the ECU. The ECU normally also controls the other actuators of the engine, monitors the health of the engine and processes sensor inputs [36].

In our setup, we override the idle speed control commands coming from the ECU with our adaptive control signal using the rapid prototyping system (see Figure 4). This system has the engine speed as the measured input and calculates the throttle command as the control input.

The existing controller on the test vehicle (which we refer to as the baseline controller) consists of a feed-forward controller in parallel with a closed loop controller of PID type. The adaptive controller overrides this feedback controller while the feed-forward controller is retained "as is". Thus our results compare the performance of the existing closed loop controller in the test vehicle with the adaptive controller.

The same adaptation gains used in the simulation shown in Fig. 3 were used for all in-vehicle experiments, without further tuning. It was observed that the Adaptive Posicast Controller performed uniformly better when compared to the existing baseline controller, in all experiments.

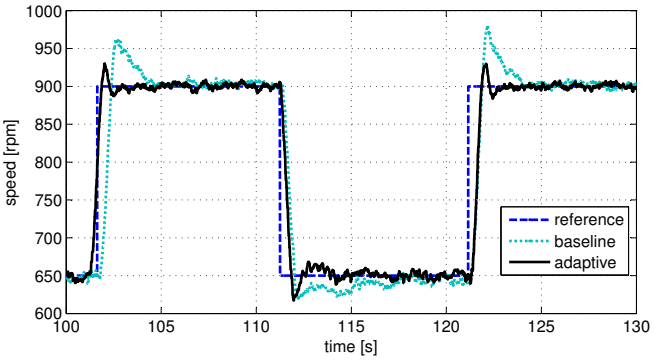

Fig. 5. Comparison of the baseline controller with adaptive controller for set-point tracking. Γ_w is the same used in the simulation shown in Fig. 3

A. *Set-point Tracking*

Figure 5 shows the set-point tracking performance for both the baseline controller and for the Adaptive Posicast Controller. This experiment was repeated for 3 minutes and the improvement over the baseline controller in RMS error was found to be 6 percent. Note that since almost always the desired idle speed is constant, the tracking is not the main concern in idle speed control.

B. *Disturbance Rejection*

We next introduced various disturbances into the picture to evaluate the disturbance rejection properties of the Adaptive Posicast Controller. Figure 6 shows the deviation from the idle speed (650 rpm) when power steering load is applied repetitively, for two different controllers. The introduction of the disturbance causes the excursions below the set-point and its release results in the ones above the set-point. This experiment was conducted for 3 minutes and the RMS error improvement over the existing baseline controller was 35 percent.

In real driving, idle speed set point may change as required to accommodate the states of accessories or changes in the battery voltage. So it is worth comparing the performance of the controllers for different operating points. Figure 7 shows the deviation from the idle speed set-point when a power steering disturbance is introduced at 900 rpm, for two different controllers. The dips correspond to the introduction of the disturbance and flares correspond to the release. This experiment was conducted for 3 minutes and RMS error improvement over the existing controller was found to be 48 percent. Similarly, Fig. 8 shows the deviation from the idle

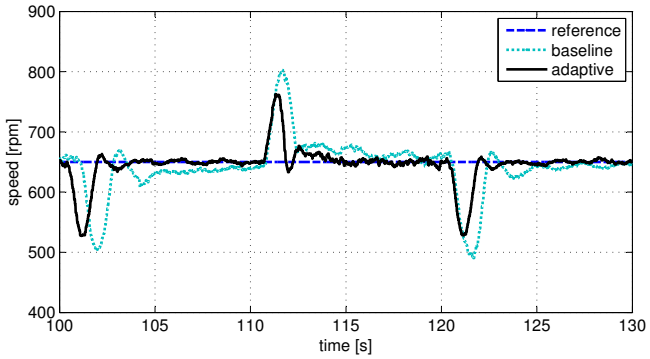

Fig. 6. Comparison of the baseline controller with adaptive controller for power steering disturbance rejection at 650 rpm. Γ_w is the same used in the simulation shown in Fig. 3

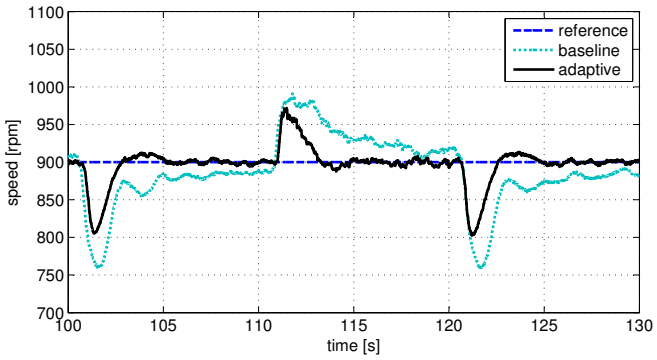

Fig. 7. Comparison of the baseline controller with adaptive controller for power steering disturbance rejection at 900 rpm. Γ_w is the same used in the simulation shown in Fig. 3

speed set-point when a power steering disturbance is introduced at 590 rpm, for two different controllers. This experiment was also conducted for 3 minutes and RMS error improvement over the existing controller was found to be 33 percent.

C. Robustness

Figure 9 shows the result of the 3-minute disturbance rejection experiment, a section of which was presented in Fig. 6. In the bottom figure of Fig. 9 the evolution of some of the adaptive parameters is presented. Note that the parameters continue to adapt during the course of the experiment and they seem to keep decreasing with a certain slope. As we discussed previously, there may be many reasons for this parameter drift, some of which can be unmodeled dynamics,

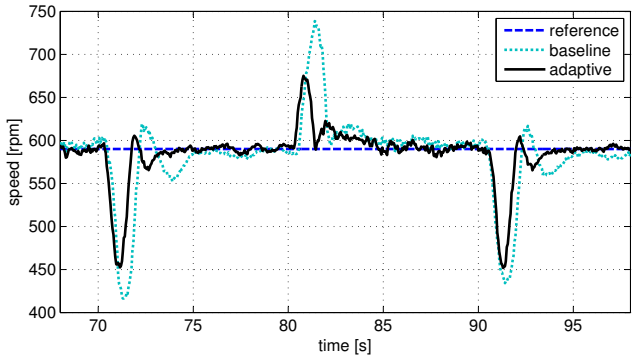

Fig. 8. Comparison of the baseline controller with adaptive controller for power steering disturbance rejection at 590 rpm. Γ_w is the same used in the simulation shown in Fig. 3

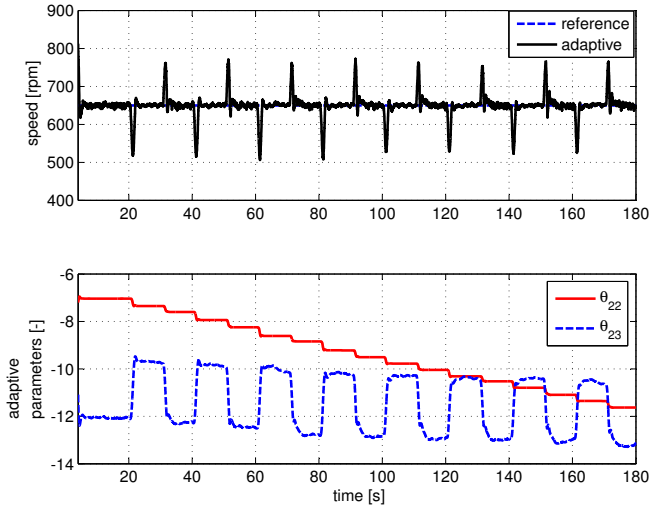

Fig. 9. Top figure: Adaptive controller performance for power steering disturbance. Bottom figure: Evolution of the controller parameters.

noise and measurement errors. Another possibility is that the parameters would converge to a bounded region after a long time period. In any case, it is not practical to apply the adaptive controller without a robustness scheme which will make sure that the parameters stay in a predetermined bounded region so that the possibility of instability is prevented.

Figure 10 presents the disturbance rejection experimental result where we applied the robustness scheme which is explained in (26). Note that the adaptive parameters continue to decrease

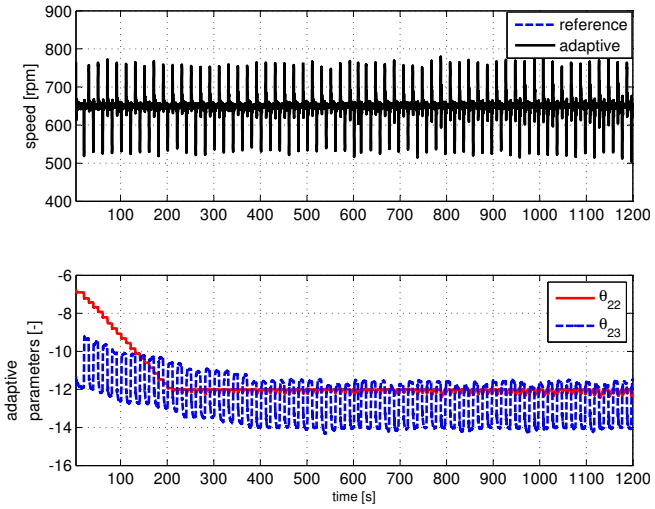

Fig. 10. Top figure: Adaptive controller performance for power steering disturbance. Bottom figure: Evolution of the controller parameters with σ-modification.

until they hit their predetermined values and then continue to adapt without leaving that region and stay bounded. An interesting point here is that although the adaptation is restricted in a certain region, the performance improvement is still more or less the same, 38 percent, as in the case without any restrictions (36 percent).

VI. Summary

We successfully applied the Adaptive Posicast Controller for time-delay systems proposed in [23] and [24] to the idle speed control (ISC) problem in an internal combustion engine. In addition to initial controller design which is presented in Section III-A, we enhanced the controller with a robustifying scheme, an adaptation rate selection algorithm, a fine-tuning procedure and an anti-windup logic, and we demonstrated the disturbance rejection properties of the controller. Note that all these enhancements are built hand in hand with the implementation since they all stemmed from the implementation requirements.

Simulations and in-vehicle experimental results confirm that performance improvements can be attained using this approach. In addition, the approach has a potential to reduce calibration time and effort due to two reasons: First, the controller performs better than the existing baseline controller which suggests that the overall controller (feed-forward + closed loop) can be designed

by relying less on the feed-forward part which consumes most of the calibration time and effort. Second, the procedure developed in Section III-B4 and III-B5 dramatically facilitates the design of the adaptive controller and minimizes the tuning process. Hence, the controller can be designed with minimum iteration which means reduced calibration time.

APPENDIX A
DISTURBANCE REJECTION PROOF

When there is a constant disturbance $d \in \Re$ present in the system, the state space description of the plant (9) is modified as

$$\dot{x}_{\rm p}(t) = A_{\rm p}x_{\rm p}(t) + b_{\rm p}(u(t-\tau)+d), \;\; y(t) = h_{\rm p}^T x_{\rm p}(t) \tag{30}$$

This, in turn, modifies the error equation (20) as

$$\begin{aligned} \dot{e}(t) &= A_{\rm m}e(t) + b_{\rm m}[\tilde{\alpha}^T(t-\tau)\omega(t-\tau) \\ &\quad + \int_{-\tau}^{0} \tilde{\lambda}(t-\tau,\sigma)u(t-\tau+\sigma){\rm d}\sigma \\ &\quad + \tilde{k}r(t-\tau) + d] \\ e_1(t) &= h_{\rm m}^T e(t). \end{aligned} \tag{31}$$

Note that in idle speed application, the idle speed reference, $r_0 \in \Re$, is constant and, therefore, we have $r(t-\tau) = r_0$ in (31). We define a new variable $\tilde{k}'$ as

$$\tilde{k}' = \tilde{k} + \frac{d}{r_0} \tag{32}$$

Hence, (31) reduces to

$$\begin{aligned} \dot{e}(t) &= A_{\rm m}e(t) + b_{\rm m}[\tilde{\alpha}^T(t-\tau)\omega(t-\tau) \\ &\quad + \int_{-\tau}^{0} \tilde{\lambda}(t-\tau,\sigma)u(t-\tau+\sigma){\rm d}\sigma \\ &\quad + \tilde{k}'r_0] \\ e_1(t) &= h_{\rm m}^T e(t). \end{aligned} \tag{33}$$

which can also be written as

$$\begin{aligned} \dot{e}(t) &= A_{\rm m}e(t) + b_{\rm m}[\tilde{\theta}'^T(t-\tau)\Omega(t-\tau) \\ &\quad + \int_{-\tau}^{0} \tilde{\lambda}(t-\tau,\sigma)u(t-\tau+\sigma){\rm d}\sigma] \\ e_1(t) &= h_{\rm m}^T e(t). \end{aligned} \tag{34}$$

where, $\tilde{\theta}' = \begin{bmatrix} \tilde{\alpha}_1 & \tilde{\alpha}_2 & \tilde{k}' \end{bmatrix}^T$. Equations (34) and (31) are exactly the same equations written using different variables, meaning that the definition of the new variable does not alter the equilibrium position of the differential equation. In addition, (34) is in the same form as in the case of disturbance free system (21), so the stability proof follows the same lines and $\lim_{t\to\infty} e_1(t) \to 0$. So, the system is stable, the disturbance is rejected and the plant output follows the reference model output asymptotically.

To conclude, disturbance rejection is achieved by eliminating the disturbance term in the error equation and this is done by introducing a new variable defined by shifting the feed-forward controller term k by a constant.

APPENDIX B
MEMORY REQUIREMENTS AND COMPUTATIONAL COMPLEXITY

Equation (14) gives the control law and the adaptation laws. Note that the finite integral term is approximated as shown in (22) and together with the λ_{i} terms introduced by this approximation we have totally 12 controller parameters. These control parameters multiplies the 12 states to form 12 terms that add up to form the control signal. In addition we need 12 terms to update the controller parameters. To calculate the update laws we also need to know the tracking error and 12 adaptation rates, together with z_{y} for the fine-tuning. For the robustness scheme, we need to store the value of σ and 12 different threshold values. Summing these up, we have totally 85 float variables that needs 340 bytes of memory space.

As for the number of operations, we have 12 multiplication operations to create the terms in the control signal, 11 sums to add up those terms, 36 multiplications for the calculation of the adaptive law terms terms and 12 additions for updating the control parameters and 12 comparisons for the robustness scheme. Totally we have 83 operations per computation cycle. With a 30 ms sampling rate of the idle speed control algorithm, we have approximately $2.8 \cdot 10^3$ flops. Assuming an average ECU speed of 10^7 flops, we need 0.028 percent of the total computational power.

APPENDIX C
STABILITY OF INTEGRAL APPROXIMATION

The closed loop system, with the controller using (22) as the integral approximation, has an unbounded sequence of characteristic roots whose accumulation points have real parts that are equal to the real parts of the roots of the following equation [34]:

$$u(t) = \lambda_1(t)u(t-dt) + .. + \lambda_m(t)u(t-mdt) \tag{35}$$

where $m = 5$. We observed in the experiments that λ_i values were in the order of 10^{-4}. Using this value as the avarage value for λ_i's and taking the Laplace transform of (35), we obtain the following characteristic equation:

$$1 - 10^{-4}\left(e^{-0.03s} + .. + e^{-0.15s}\right) = 0 \tag{36}$$

It is obvious that the characteristic roots can not have positive real parts. Referring the average value of λ_i's as λ_{avg} and considering the case where the characteristic roots are on the jw axis, so the real parts of the roots are 0, we obtain that

$$1 - \lambda_{\text{avg}}\left(e^{-0.03\text{j}\beta} + .. + e^{-0.15\text{j}\beta}\right) = 0 \tag{37}$$

where jβ refers to the imaginary part of the characteristic root. Note that for $\beta = 0$, (37) is satisfied if $\lambda_{\text{avg}} = 0.2$. Therefore, unless $\lambda_{\text{avg}} \geqslant 0.2$, (37) can not be satisfied and hence all the roots remain in the left half complex plane. This means that even if the observed values of λ_i's were $0.2/10^{-4} = 2000$ times larger, we would still have an integral approximation that would yield a stable closed loop system.

ACKNOWLEDGMENT

This work was supported through the Ford-MIT Alliance Initiative. The authors would like to acknowledge Dr. Davor Hrovat of Ford Motor Company for his support and encouragement during this project, and Chris Teslak of Ford Motor Company for help with the experimental setup in the vehicle. The authors also wish to acknowledge Dr. Alex Gibson of Ford Motor Company for valuable discussions.

REFERENCES

[1] D. Hrovat and J. Sun, "Models and control methodologies for ic engine idle speed control design," *Control Eng. Practice*, vol. 5, no. 8, pp. 1093–1100, 1997.

[2] S. J. Williams *et al*, "Idle speed control design using an H_∞ approach," in *Proc. Amer. Control Conf.*, 1989, pp. 1950–1956.

[3] R. D. Filippi and R. Scattolini, "Idle speed control of a F1 racing engine," *Control Eng. Practice*, vol. 14, no. 3, pp. 251–257, 2005.

[4] L. Kjergaard, S. Nielsen, T. Vesterholm, and E. Hendricks, "Advanced nonlinear engine idle speed control systems," in *Proc. of SAE*, no. 940974, 1994.

[5] X. Li and S. Yurkovich, "Sliding mode control of delayed systems with application to engine idle speed control," *IEEE Transactions on Control Systems Technology*, vol. 9, no. 6, pp. 802–810, Nov. 2001.

[6] K. R. Butts, N. Sivashankar, and J. Sun, "Application of ℓ_1 optimal control to the engine idle speed control problem," *IEEE Transactions on Control Systems Technology*, vol. 7, no. 2, pp. 258–270, 1999.

[7] T.-L. Chien, C.-C. Chen, and C.-Y. Hsu, "Tracking control of nonlinear automobile idle-speed time-delay system via differential geometry approach," *Journal of the Franklin Institute*, vol. 342, no. 7, pp. 760–775, Nov. 2005.

[8] P. K. Kokotovic and D. Rhode, "Sensitivity guided design of an idle speed controller," Ford Motor Company, PK Research, Urbana, U.S.A., Technical Report 1, 1986.

[9] A. Gangopadhyay and P. Meckl, "Multivariable pi tuning and application to engine idle speed control," in *Proc. Amer. Control Conf.*, San Diego, CA, June 1999, pp. 2678–2682.

[10] J. Grizzle, J. Buckland, and J. Sun, "Idle speed control of a direct injection spark ignition stratified charge engine," *Int. J. Robust Nonlinear Control*, vol. 47, no. 1, pp. 17–23, 1988.

[11] S. Yurkovich and M. Simpson, "Crank-angle domain modeling and control for idle speed," *SAE Paper*, no. 970027, 1997.

[12] Y. Wang, A. Stefanopoulou, and M. Levin, "Idle speed control: An old problem in a new engine design," in *Proc. Amer. Control Conf.*, San Diego, CA, June 1999, pp. 1217–1221.

[13] B. K. Powell and W. F. Powers, "Linear quadratic control design for nonlinear ic engine systems," in *Proc. of ISATA Conference*, Stockholm, Sweden, 1981.

[14] G. D. Nicolao, C. Rossi, R. Scattolini, and M. Suffritti, "Identification and idle speed control of internal combustion engines," *Control Eng. Practice*, vol. 7, no. 9, pp. 1061–1069, Sep. 1999.

[15] D. Hrovat, "MPC-based idle speed control for IC engine," in *Proc. of FISITA conference*, Prague, Czech Rep., 1996.

[16] W. P. Mihelc and R. D. Citron, "An adaptive idle speed mode control design," in *Proc. of SAE*, no. 840443, 1981.

[17] D. Kim and J. Park, "Application of adaptive control to the fluctuation of engine speed at idle," *Information Sciences*, vol. 177, no. 16, pp. 3341–3355, Aug. 2007.

[18] F.-C. Hsieh, B.-C. Chen, and Y.-Y. Wu, "Adaptive idle speed control for spark-ignition engines," *SAE Paper*, no. 2007-01-1197, 2007.

[19] A. Stotsky, B. Egardt, and S. Eriksson, "Variable structure control of engine idle speed with estimation of unmeasurable disturbances," *Journal of Dynamic Systems, Measurement and Control*, vol. 122, no. 4, pp. 599–603, 2000.

[20] D. Pavkovi, J. Deur, V. Ivanovi, and D. Hrovat, "SI engine load torque estimator based on adaptive kalman filter and its application to idle speed control," *SAE Paper*, no. 2005-01-0036, 2005.

[21] S. Niwa and M. Kajitani, "High performance idle speed control applying the disturbance cancellation control," *SAE Paper*, no. 2003-08-0392, 2003.

[22] M. Thornhill, S. Thompson, and H. Sindano, "A comparison of idle speed control schemes," *Control Eng. Practice*, vol. 8, no. 5, pp. 519–530, May 2000.

[23] S.-I. Niculescu and A. M. Annaswamy, "An adaptive smith-controller for time-delay systems with relative degree $n^* \leqslant 2$," *Systems and Control Letters*, vol. 49, pp. 347–358, 2003.

[24] Y. Yildiz, A. Annaswamy, I. Kolmanovsky, and D. Yanakiev, "Adaptive posicast controller for time-delay systems with relative degree $n^* \leqslant 2$," *under review*, http://web.mit.edu/aaclab/publications/index.html.

[25] Y. Yildiz, A. Annaswamy, D. Yanakiev, and I. Kolmanovsky, "Adaptive idle speed control for internal combustion engines," in *Proc. Amer. Control Conf.*, New York City, July 2007, pp. 3700–3705.

[26] ——, "Automotive powertrain control problems involving time delay: An adaptive control approach," in *Proc. of ASME Dynamic Systems and Control Conference*, Ann Arbor, Michigan, Oct. 2008.

[27] ——, "Adaptive air fuel ratio control for internal combustion engines," in *Proc. Amer. Control Conf.*, Seattle, Washington, June 2008, pp. 2058–2063.

[28] O. J. Smith, "A controller to overcome dead time," *ISA Journal*, vol. 6, 1959.

[29] A. Z. Manitius and A. W. Olbrot, "Finite spectrum assignement problem for systems with delays," *IEEE Transactions on Automatic Control*, vol. 24, no. 4, 1979.

[30] K. Ichikawa, "Frequency-domain pole assignement and exact model-matching for delay systems," *International Journal of Control*, vol. 41, pp. 1015–1024, 1985.

[31] R. Ortega and R. Lozano, "Globally stable adaptive controller for systems with delay," *International Journal of Control*, vol. 47, no. 1, pp. 17–23, 1988.

[32] L. Guzzella and C. H. Onder, *Introduction to Modeling and Control of Internal Combustion Engine Systems*, 1st ed. Springer, 2004.

[33] K. S. Narendra and A. M. Annaswamy, *Stable adaptive systems*. New York: Dover Publications, 2005.

[34] K. Engelborghs, M. Dambrine, and D. Roose, "Limitations of a class of stabilization methods for delay systems," *IEEE Trans. Automatic Control*, vol. 46, no. 2, Feb. 2001.

[35] S. P. Karason and A. M. Annaswamy, "Adaptive control in the presence of input constraints," *IEEE Trans. Automatic Control*, vol. 39, no. 11, pp. 2325–2330, Nov. 1994.

[36] M. J. van Nieuwstadt, I. V. Kolmanovsky, P. E. Moraal, A. Stefanopoulou, and M. Jankovic, "EGR-VGT control schemes: experimental comparison for a high-speed diesel engine," *IEEE Control Systems Magazine*, vol. 20, no. 3, pp. 63–79, Jun. 2000.